Torocyte Membrane Endovesicles Induced by Octaethyleneglycol Dodecylether in Human Erythrocytes

Malgorzata Bobrowska-Hägerstrand,* Veronika Kralj-Iglič,# Aleš Iglič,§ Katarzyna Bialkowska,¶ Boris Isomaa,* and Henry Hägerstrand*

*Department of Biology, Åbo Akademi University, FIN-20520, Åbo/Turku, Finland; #Institute of Biophysics, Medical Faculty, University of Ljubljana, SI-1000 Ljubljana, Slovenia; §Laboratory of Applied Physics, Faculty of Electrical Engineering, SI-1000 Ljubljana, Slovenia; and ¶Institute of Biochemistry, University of Wroclaw, PL-51148 Wroclaw, Poland

ABSTRACT Endovesicles induced in human erythrocytes by octaethyleneglycol dodecylether (C12E8) were studied by confocal laser scanning microscopy, using fluorescein isothiocyanate dextran as a nonspecific fluid marker. The endovesicles appeared to consist mainly of a ring-formed toroidal part joined with a central flat membrane segment. The torocyte contour length was several μm. There was usually one torocyte endovesicle per cell. The endovesicles seemed to be located near the cell surface. In sections of C12E8-treated erythrocytes transmission electron microscopy revealed the frequent occurrence of flat membrane structures with a bulby periphery, which apparently are cross sections of torocyte endovesicles. The possible physical mechanisms leading to the observed torocyte endovesicle shape are discussed. The torocyte endovesicles seem to be formed in a process in which an initially stomatocytic invagination loses volume while maintaining a large surface area. Because intercalation of C12E8 in the erythrocyte membrane induces inward membrane bending (stomatocytosis) we assume that C12E8 is preferentially located in the inner lipid layer of the erythrocyte membrane, i.e., in the outer lipid layer of the endovesicle membrane. It is suggested that local disturbances of the lipid molecules in the vicinity of the C12E8 molecules in the outer lipid layer of the endovesicle membrane form membrane inclusions with the effective shape of an inverted truncated cone. If the interaction between the inclusion and the membrane is weak, the membrane of such an endovesicle can be characterized by its negative spontaneous curvature, which may lead to a torocyte endovesicle shape with a small relative volume. Effects of a possible strong interaction between the C12E8-induced membrane inclusions and the membrane on the stability of the torocyte endovesicles are also indicated.

INTRODUCTION

We have previously reported that the patterns whereby different stomatocytogenic water-soluble amphiphiles induce membrane invaginations and endovesicles in human erythrocyte may differ (Hägerstrand and Isomaa, 1989, 1992). By means of transmission electron microscopy (TEM) and fluorescence microscopy it was observed that many stomatocytogenic amphiphiles (for example, chlorpromazine hydrochloride) induce small spherical endovesicles in erythrocytes. The stomatocytogenic detergent polyethyleneglycol dodecylether (C12E8), however, induces endovesicles with a unique puzzling ring-like shape. In the present study we used confocal laser scanning microscopy (CLSM) in combination with the nonspecific fluid-phase marker fluorescein isothiocyanate (FITC-dextran) and TEM to study the morphology and localization of the C12E8-induced membrane endovesicles. Furthermore, scanning electron microscopy (SEM) was used to characterize the shape transformation induced by C12E8. We discuss molecular features of C12E8 that may be important for the formation of the torocyte endovesicles and discuss the possible physical mechanism for their formation.

Received for publication 30 June 1998 and in final form 24 August 1999.

Address reprint requests to Dr. Henry Hägerstrand, Department of Biology, Åbo Akademi University, Biocity, FIN-20520 Åbo/Turku, Finland. Tel.: 358-2-2154089; Fax: 358-2-2154748; E-mail: henry.hagerstrand@aton.abo.fi.

0006-3495/99/12/3356/07 $2.00

MATERIALS AND METHODS

Chemicals

C12E8 (74680) was purchased from Fluka; chlorpromazine hydrochloride (C-8138) and FITC-dextran (FD-70S) were from Sigma.

Treatment with C12E8

Blood was drawn from the authors by venipuncture into heparinized tubes. The erythrocytes were washed three times in a buffer containing 145 mM NaCl, 5 mM KCl, 4 mM Na_2HPO_4, 1 mM NaH_2PO_4, 1 mM $MgSO_4$, 1 mM $CaCl_2$, and 10 mM glucose (pH 7.4) and subsequently suspended in the buffer at a cell density of 1.65×10^9 cells/ml. Experiments were performed within 24 h after the blood was drawn. Aliquots of a prewarmed (37°C) erythrocyte stock suspension were pipetted into Eppendorf tubes containing prewarmed (37°C) FITC-dextran (10 mg/ml; Sigma) in buffer with and without C12E8. The final cell density was 1.65×10^8 cells/ml ($\simeq$1.5% hematocrit), and the incubation was carried out for 60 min.

Confocal laser scanning microscopy

After treatment with C12E8, cells were washed three times and incubated in glutaraldehyde (0.5%) for 30 min at room temperature. After 2 washes 10 ml of cell suspension was allowed to dry ($\simeq$1 h) on a coverslip. Within 10 min after the blood smear was visually dry, 5 μl Mowiol (40–88; Aldrich) was applied to the smear, and the coverslip was placed on an object glass. After some hours the sample was sealed with nail polish and kept at 4°C until studied.

Samples were studied (100×/1.4 aperture immersion oil objective, 10× ocular) and scanned ($\simeq$0.05 mm between scanned sections), using a Leica confocal laser scanning microscope. Scans were combined to images giving maximum projection. The best three-dimensional information was

obtained by rotation of the three-dimensional images. For Fig. 1 images were handled in Adobe software program and printed via Corel-draw software program.

Transmission electron microscopy

After treatment with C12E8, erythrocytes were suspension-fixed in 1% glutaraldehyde in the buffer for 30 min at 22°C, postfixed in 1% OsO_4 in 0.9% NaCl for 30 min at 22°C, dehydrated in a graded series of acetone/water (50–100%, w/w), and finally embedded in Epon. The sections were stained with lead acetate and poststained with uranyl acetate before examination in a JOEL 100SX electron microscope.

Scanning electron microscopy

Erythrocytes, fixed, postfixed, and dehydrated as above, were critical-point dried, gold-sputtered, and finally examined in a Cambridge Instruments S360 microscope.

EXPERIMENTAL RESULTS

Human erythrocytes were incubated, in the presence of FITC-dextran (10 mg/ml), (37°C, 60 min) with C12E8. After glutaraldehyde fixation, cells were studied by confocal laser scanning microscopy. The fluorescence caused by glutaraldehyde in the cell membrane served for orientation. This was especially favorable when three-dimensional information was collected by rotating the image.

Untreated erythrocytes (control) showed no enclosed FITC-dextran (Fig. 1 *A*). At a high sublytic C12E8 concentration (44 μM) 5–20% of erythrocytes developed FITC-dextran-containing structures. There was usually one fluorescent structure per cell. The structure most frequently appeared to have a ring-like toroidal part and a central plate-like part (Fig. 1 *B*). This shape is referred to as the torocyte shape (Deuling and Helfrich, 1976). The toroid contour was usually several μm long. Occasionally, small torocyte or tubular structures occurred.

That the FITC-dextran-containing torocyte structures persisted through extensive washing, several days of storage, and cell lysis (not shown) indicates that the structures are endovesicles and not open invaginations. Large open connections between the FITC-dextran-containing structures and the surroundings would cause a depletion of FITC-dextran after washing and storage. The structures are therefore called endovesicles, although it cannot be excluded that there is a tiny neck forming a connection between the solution within the endovesicle and the outer solution of the cell. However, no such connections were seen. The accumulation of FITC-dextran in the endovesicles is not due to a specific binding of fluorescein to membrane components, because similarly shaped endovesicles were seen when rhodamine B isothiocyanate-conjugated dextran was used (not shown).

Rotation of the three-dimensional image indicated that the endovesicles were located close to the inside of the cell membrane. At incubations shorter than 30 min endovesicles were less abundant, torocyte endovesicles had a smaller

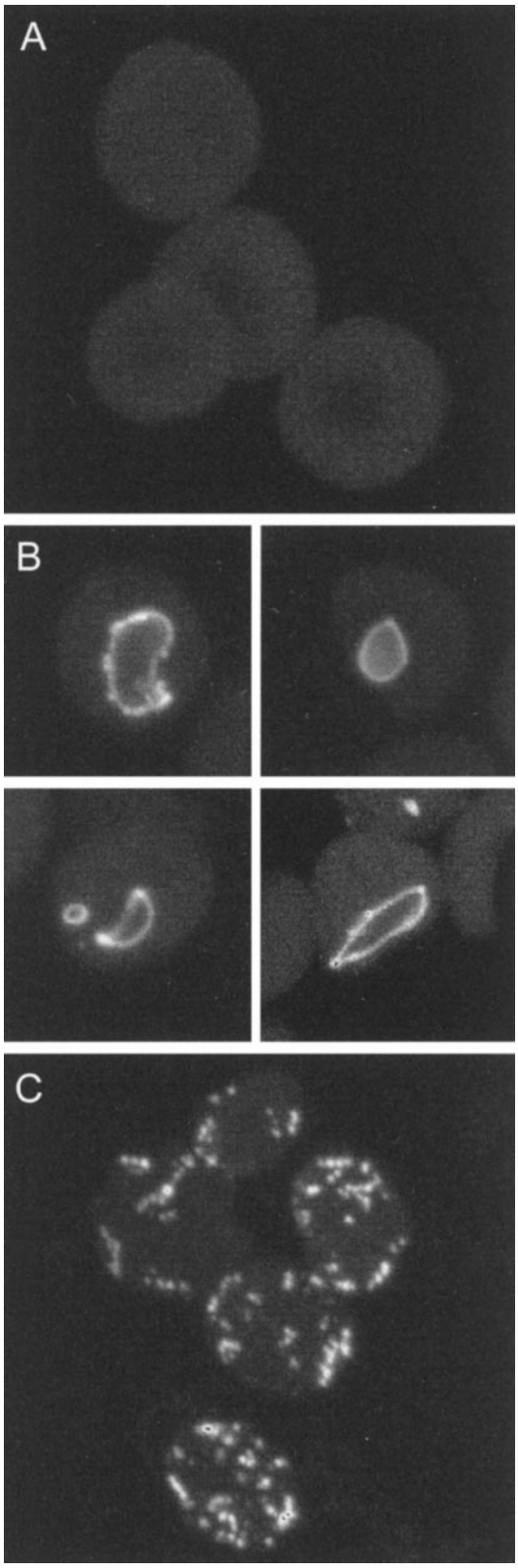

FIGURE 1 Confocal laser scanning microscopy (maximum projection images) of human erythrocytes incubated (60 min, 37°C) with amphiphiles at sublytic concentrations in the presence of FITC-dextran (10 mg/ml). Images have approximately a similar magnification. (*A*) Control. (*B*) Erythrocytes treated with C12E8 (44 μM); toroidal endovesicles. (*C*) Erythrocytes treated with chlorpromazine (100 mM); small spherical endovesicles.

diameter, and tube-like endovesicles occurred more often (not shown). At a low sublytic concentration (22 μM) endovesicles were rarely observed. Experiments with the C10, C14, and C16 homologs of C12E8 at high sublytic concentrations showed that they may also induce torocyte endovesicles.

TEM studies of sections of erythrocytes treated with C12E8 (44 μM, 37°C, 60 min) revealed the frequent occurrence of large flat invaginations/endovesicles, often with a compressed central area and a bulby periphery (Fig. 2). Similar endovesicles were induced by the C10, C14, and C16 homologs of C12E8 at high sublytic concentrations.

SEM studies revealed pocket-like cavities on erythrocytes incubated for 5–15 min with C12E8 (44 mM). In addition, strong bending and twisting of the cells also seemed to occur (Fig. 3, *B* and *C*). After a 30-min incubation erythrocytes mainly had a rounded shape (Fig. 3 *D*).

To conclude, CLSM images show that the fluorescence is much more intensive at the edge of the C12E8-induced endovesicle than in its central part, indicating that the endovesicles consist of a tube-like periphery and a thin flat central area. This interpretation is in good agreement with the results of the TEM studies (Fig. 2). The torocyte character of the C12E8-induced endovesicles is also consistent

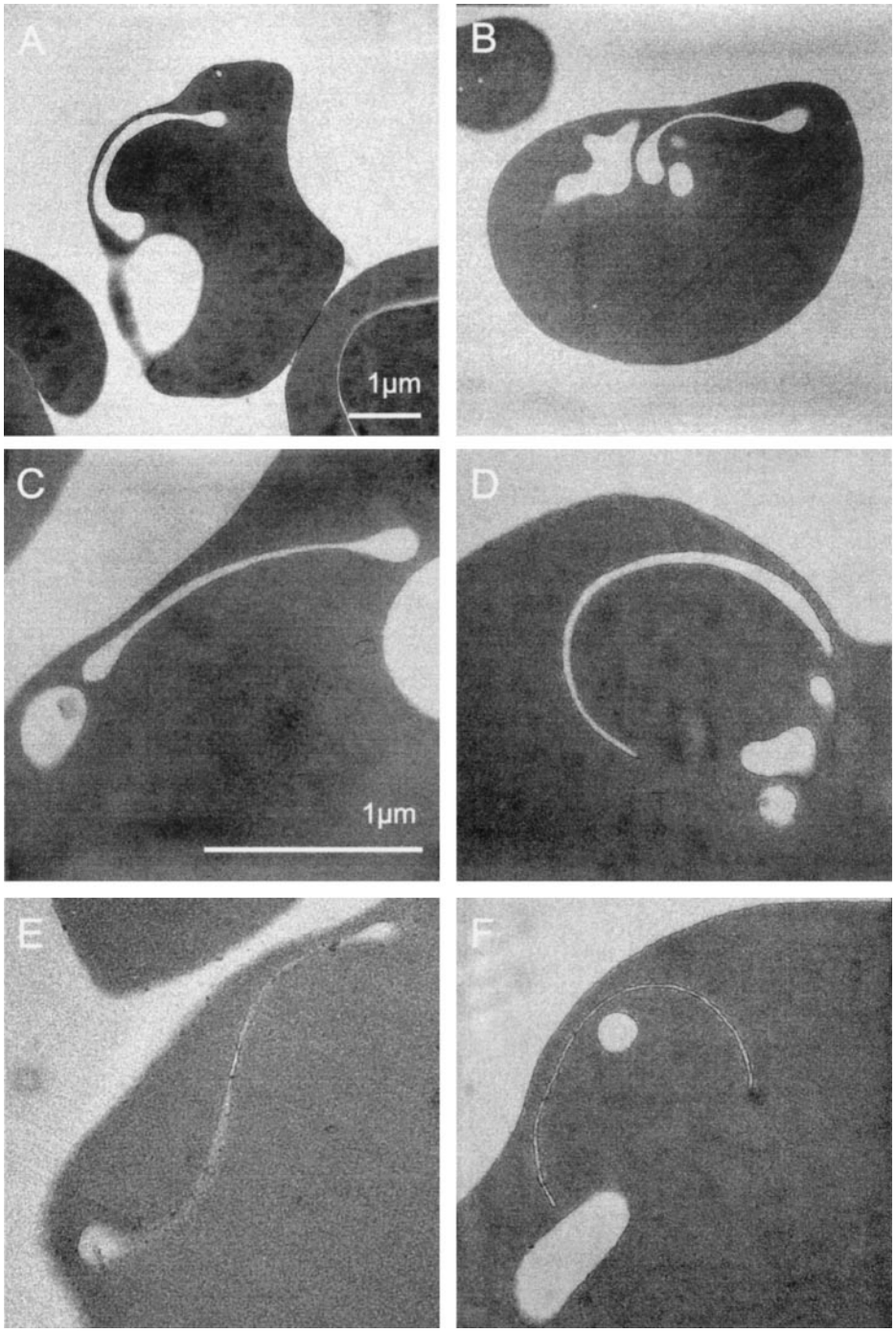

FIGURE 2 TEM micrographs showing human erythrocytes incubated with C12E8 (44 μM, 60 min, 37°C). Note the plate-like invaginations/endovesicles eventually having bulby ends. For *A* and *B* see bar in *A*; for *C–F* see bar in *C*.

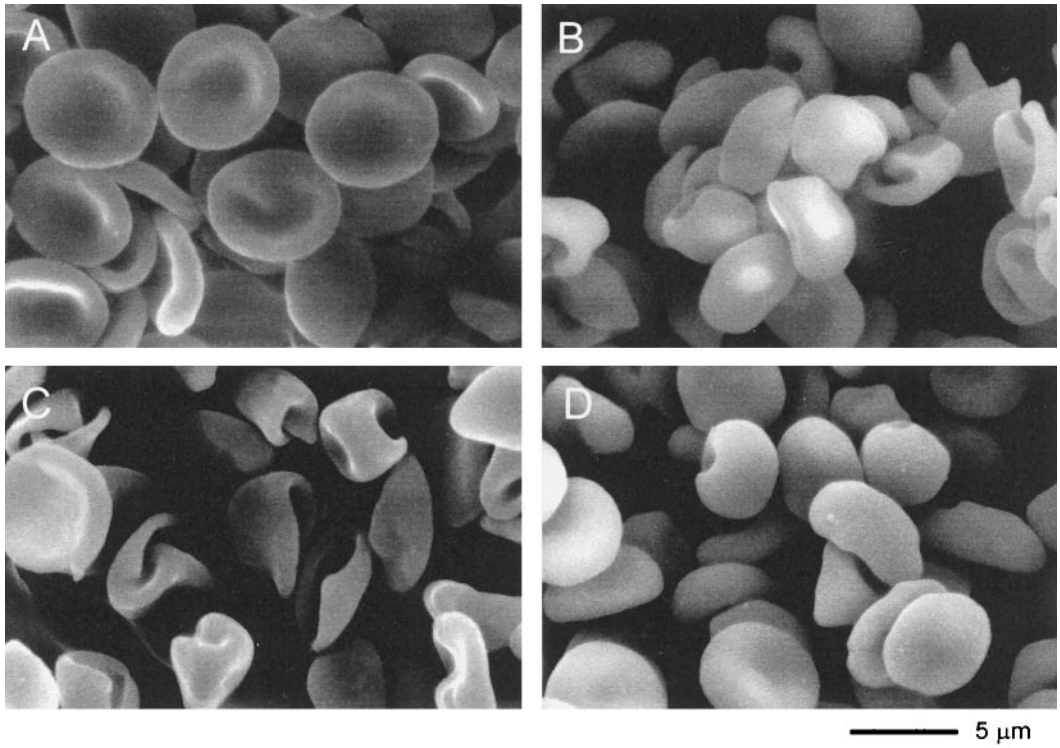

FIGURE 3 SEM micrographs showing shape transformations in human erythrocytes induced by C12E8 (44 μM, 37°C): 0 min (*A*), 5 min (*B*), 15 min (*C*), and 30 min (*D*).

with the SEM images if one assumes that torocyte endovesicles are formed in a process in which an initially stomatocytic invagination loses volume while maintaining its large surface area (Fig. 3).

The C12E8-induced stomatocyte transformation differs in some respects from the shape transformation induced by chlorpromazine, the reference compound in this study. In the chlorpromazine-treated erythrocytes no bended or twisted cell shapes were observed. Upon chlorpromazine treatment cells immediately become cup-shaped and finally attain an appearance close to a spherical shape (Deuticke, 1968; Sheetz and Singer, 1974, 1976; Fujii et al., 1979; Isomaa et al., 1987). In the final stage the cells contain many small spherical endovesicles that seem to be mainly formed in the membrane domain of the initial large invagination (Hägerstrand and Isomaa, 1989, 1991, 1992). Accordingly, in the present study, chlorpromazine (100 mM, 37°C, 60 min) was shown to mainly induce small spherical endovesicles close to the cell membrane (Fig. 1 *C*), and these endovesicles were observed in all cells.

THEORETICAL DISCUSSION

By intercalating into the erythrocyte membrane the C12E8 molecule perturbs the membrane structure, e.g., it causes a change in packing of the lipid molecules (Heerklotz et al., 1998). As a consequence, a C12E8-induced inclusion may be formed in the membrane. We define a C12E8 membrane inclusion as a complex composed of the embedded C12E8 molecule and some adjacent phospholipid molecules (Heerklotz et al., 1998), which are significantly distorted because of the presence of the embedded C12E8 molecule. Based on experimental data (Thurmond et al., 1994; Heerklotz et al., 1997), we assume that the inclusion formed by the C12E8 molecule has the effective shape of an inverted truncated cone (see Appendix).

At present we do not have experimental evidence about the strength of the interaction between the C12E8 inclusion and the surrounding membrane. Therefore we will indicate the possible mechanisms that may lead to the observed torocyte endovesicle, involving the limit of weak interaction and the limit of strong interaction between the C12E8 inclusion and the surrounding membrane. The free energy of the membrane inclusions with the limits of weak and strong interaction is briefly described in the Appendix.

If the interaction energy between the C12E8 inclusion and the surrounding membrane is small compared to kT and if the mean curvature of the intrinsic shape of the inclusion $\bar{C}_m$ (see Appendix) is much larger than the mean curvature attained by the membrane $\bar{C} = (C_1 + C_2)/2$, the correction of the spontaneous curvature of the membrane C_o due to membrane-embedded inclusions is (Kralj-Iglič et al., 1999)

$$\bar{C}_o \cong C_o + \xi M_T \bar{C}_m / 2Ak_c, \quad (1)$$

where M_T is the total number of inclusions embedded in the membrane, ξ is the interaction constant (see Appendix), A is the membrane area, C_1 and C_2 are the principal membrane

curvatures, and k_c is the local bending modulus of the membrane (Evans and Skalak, 1980).

Because intercalation of C12E8 into the erythrocyte membrane induces inward membrane bending (stomatocytosis) (Fig. 3) we assume that C12E8 is preferentially located in the inner erythrocyte membrane layer (Sheetz and Singer, 1974; Iglič and Hägerstrand, 1999; Waugh, 1996).

In the endovesicle, the inner layer of the cell membrane is on the outer side. Therefore with respect to such an endovesicle, the C12E8 inclusions are distributed in the outer layer of the endovesicle. Taking into account that the inclusions have the shape of the inverted truncated cone ($\bar{C}_m < 0$), the spontaneous curvature of the endovesicle membrane $\bar{C}_o$ decreases with increasing number of intercalated C12E8 molecules, which may lead to negative spontaneous curvature of the endovesicle membrane. Negative spontaneous curvature of the endovesicle membrane may favor torocyte endovesicle shapes, because in these shapes there are relatively large regions with low or negative membrane mean curvature $\bar{C}$.

In contrast, the preferential intercalation of chlorpromazine molecules into the inner layer of the erythrocyte membrane (the outer layer of the endovesicle membrane) (Sheetz and Singer, 1974) increases the spontaneous curvature of the endovesicle membrane probably because of the conical shape of chlorpromazine ($\bar{C}_m > 0$) (see also Israelachvili, 1985). The large positive spontaneous curvature of the endovesicle membrane favors a large curvature of the endovesicle membrane, which can be accomplished by forming many small spheres. Indeed, if erythrocytes are treated with chlorpromazine, they reach the limiting shape composed of a nearly spherical mother cell and many more or less spherical endovesicles with very high membrane mean curvature (Fig. 1 *C*).

The effective shape of C12E8 inclusions may also influence the shape of the endovesicle by affecting the Gaussian modulus (Fischer, 1992, 1993) of the membrane (Fournier, 1996; Kralj-Iglič et al., 1999). This might also be a part of the selective mechanism that determines whether in the final state the parent cell will have many small daughter vesicles or the opposite, as few daughter vesicles as possible. The former situation could correspond to the effect of chlorpromazine, while the latter could result from insertion of C12E8.

If the interaction between the inclusion and the membrane is on the order of kT or larger, the lateral distribution of the inclusions is nonhomogeneous (Markin, 1981; Leibler, 1986; Andelman et al., 1992; Seifert, 1993; Kralj-Iglič et al., 1996; Boulbitch, 1997). If the inclusions are, in addition, anisotropic, i.e., nonaxisymmetric with respect to the membrane normal vector, they also exhibit the orientational ordering in the plane of the membrane according to the local difference between the two principal curvatures (the curvature deviator) (Fournier, 1996; Kralj-Iglič et al., 1999). These effects may considerably influence the cell shape (see Appendix). It was indicated that the torocyte shape corresponds to a large average curvature deviator, which may give low membrane free energy (Iglič et al., 1998).

SUMMARY AND CONCLUSIONS

It is suggested that the effective molecular shape of the C12E8 membrane inclusions, where each inclusion consists of the intercalated exogenously added molecule C12E8 and distorted neighbor phospholipids (Thurmond et al., 1994; Otten et al., 1995; Heerklotz et al., 1997), are essential for the torocyte shape of endovesicles. The molecular features of C12E8 responsible for its capacity to induce torocyte and occasionally cylindrical endovesicles may be looked for by comparing its molecular features with those of stomatocytic amphiphiles, which induce small spherical endovesicles.

Stomatocytogenic amphiphiles, not only charged species like chlorpromazine and bile acids, but also the nonionic Triton X-100, induce small spherical endovesicles in erythrocytes (Hägerstrand and Isomaa, 1989, 1991, 1992). This shows that the tendency of C12E8 to form torocyte endovesicles is not simply related to its nonionic character. C12E8 and Triton X-100 have a largely similar hydrophilic headgroup—a polyethylene chain. However, while Triton X-100 has a bulky phenol ring in its hydrophobic part, C12E8 bears a straight alkyl chain. This could be taken to indicate that the difference in the volumes of their hydrophobic groups may be relevant to the shape of the invaginations and endovesicles induced. However, a small hydrophobic volume of a nonionic amphiphile is apparently not enough to induce torocyte endovesicles, because octyl- and decylglucopyranosides, which bear a straight hydrophobic alkyl chain (and a bulky hydrophilic group), do not induce torocyte endovesicles. Instead, they cause a formation of a necklace of small spherical endovesicles (Hägerstrand and Isomaa, 1992). Thus it appears that both the hydrophilic and hydrophobic parts of C12E8, probably as expressed in its overall molecular shape (Israelachvili, 1985), may be essential in the capacity of C12E8 to induce torocyte endovesicles. Experimental observations showing that octylglucopyranoside perturbs only the acyl chain region of phosphatidiylcholine bilayers, while C12E8 perturbs both the lipid headgroup region and the acyl chain region (Otten et al., 1995; Wenk et al., 1997), may be taken to support this assumption. Specific cooperative interactions of C12E8 with the neighbor lipid and water molecules (Heerklotz et al., 1998) may be reflected in its effective molecular shape and may be responsible for the tendency of C12E8 to form torocyte endovesicles.

To summarize: our results indicate that the torocyte endovesicles originate from a primary large stomatocytic invagination that loses volume, resulting in an invagination with a large surface area but a small enclosed volume. The invagination may finally close, forming an inside-out endovesicle. Possible explanations of the observed stable shape of the endovesicles were indicated in terms of the effective shape of the C12E8 membrane inclusions. To

present a more complete view of the physical mechanism, additional experiments should be performed to determine the properties of the inclusion formed by C12E8 molecules as well as the lateral and transmembrane distributions of the intercalated C12E8 molecules.

APPENDIX: FREE ENERGY OF MEMBRANE INCLUSIONS

The properties of the C12E8 inclusion depend on the molecular shape of the intercalated C12E8 molecule and its interaction with the surrounding lipids. It has been shown that a C12E8 molecule perturbs the conformational state of the neighbor phospholipid molecules, mainly because of dehydration of their hydrophilic headgroups (Thurmond et al., 1994; Heerklotz et al., 1997, 1998). Because the acyl chains of the individual phospholipid molecules in the neighborhood of C12E8 are moved apart sideways (Thurmond et al., 1994), the average acyl chain length of the phospholipid molecule shortens while its average area increases (Otten et al., 1995). Consequently, the effective shape of the surrounding phospholipid molecules changes from a cylinder to an inverted truncated cone (Thurmond et al., 1994; Heerklotz et al., 1997). Based on these experimental data, we assume that the inclusion formed by the C12E8 molecule is an inverted truncated cone as well.

The energy of the single inclusion expresses a mismatch between the intrinsic shape of the inclusion and the local membrane shape (Kralj-Iglič et al., 1999):

$$E(\omega) = \xi(\bar{C} - \bar{C}_m)^2/2 + (\xi + \xi^*) \cdot (\hat{C}^2 - 2\hat{C}\hat{C}_m \cos(2\omega) + \hat{C}_m^2)/4, \quad \text{(A1)}$$

where ξ and ξ^* are the constants representing the strength of the interaction, $\bar{C} = (C_1 + C_2)/2$, $\bar{C}_m = (C_{1m} + C_{2m})/2$, $\hat{C} = (C_2 - C_1)/2$, $\hat{C}_m = (C_{2m} - C_{1m})/2$, C_1 and C_2 are the principal membrane curvatures, C_{1m} and C_{2m} are the principal curvatures of the intrinsic shape of the inclusion, and ω is the orientation of the principal axis system of the inclusion with respect to the local principal axis system of the membrane. If $C_{1m} = C_{2m}$ the inclusion is isotropic, while if $C_{1m} \neq C_{2m}$ the inclusion is anisotropic.

The free energy of all of the inclusions in a closed membrane layer, obtained by using the single-inclusion energy (Eq. A1) is (Kralj-Iglič et al., 1999)

$$F_m = -M_T kT \ln\left(\frac{1}{A}\int \exp(-\xi(\bar{C} \pm \bar{C}_m)^2/2kT - (\xi + \xi^*)(\hat{C}^2 + \hat{C}_m^2)/4kT) I_o((\xi + \xi^*)\hat{C}\hat{C}_m/2kT)\mathrm{d}A\right), \quad \text{(A2)}$$

where M_T is the total number of inclusions in the layer, k is the Boltzmann constant, T is the temperature, dA is the membrane area element, and I_o is the modified Bessel function obtained by integration within the partition function of a single inclusion over all possible orientations (Kralj-Iglič et al., 1999). The integration in Eq. A2 is performed over the entire membrane area A. The sign $\pm$ denotes the choice of the inner/outer membrane area.

If the interaction energy between the inclusion and the surrounding membrane is small compared to kT, the exponential and the logarithmic functions in Eq. A2 can be expanded. The inclusions are distributed over the membrane almost homogeneously, while their orientational ordering is almost random. If, furthermore, at least one of the intrinsic curvatures of the inclusion C_{1m}, C_{2m} is much larger that any of the curvatures attained by the membrane C_1, C_2, the obtained free energy of the inclusions renormalizes the constants of the standard membrane elastic energy (see Eq. 1) (Kralj-Iglič et al., 1996, 1999).

An interesting effect may be caused if the inclusions are anisotropic and strongly interact with the membrane. This is fulfilled in the regions of the membrane where the difference between C_1 and C_2 (the curvature deviator) is large. In this case the inclusions exhibit orientational ordering within the membrane plane (Fournier, 1996; Kralj-Iglič et al., 1999). We say that the membrane exhibits deviatoric properties (Fischer, 1992, 1993; Fournier, 1996). It has been suggested (Fournier, 1996; Safinya, 1997; Fournier and Galatola, 1997; Kralj-Iglič et al., 1999) that the stable cylindrical structures could not be predicted within the standard membrane elastic energy models (Evans and Skalak, 1980; Svetina and Žekš, 1989; Lipowsky, 1991; Miao et al., 1994; Svetina et al., 1994) and that the orientational ordering of anisotropic inclusions may provide a plausible explanation for the observed cylindrical shapes by favoring shapes of the large average curvature deviator. It has recently been indicated that the average curvature deviator is also large in torocyte vesicles (Iglič et al., 1998).

However, at present, no specific data on the values of the model parameters ξ, ξ^*, C_{1m}, and C_{2m} are available for C12E8 inclusions, so we cannot make a definite prediction of how C12E8 inclusions affect the cell shape and the observed endovesiculation process. A definite answer could not be given without additional experiments regarding the strength and the nature of the interaction between the C12E8 inclusion and the membrane.

We are indebted to Gunilla Henriksson and Diana Toivola for performing the venipunctures, and to Tomas Bymark and Esa Nummelin for help with preparing the figures. We thank Bojan Božič for useful discussions.

We are also indebted to the Oskar Öflund Foundation, the Research Institute and the Rector at the Åbo Akademi University, the Nessling Foundation, and the Rector at the University of Ljubljana for their financial support.

REFERENCES

Andelman, D., T. Kawakatsu, and K. Kawasaki. 1992. Equilibrium shape of two-component unilamellar membranes and vesicles. *Europhys. Lett.* 19:57–62.

Boulbitch, A. A. 1997. Crystalization of proteins accompanied by formation of cylindrical surface. *Phys. Rev. E.* 56:3395–3400.

Deuling, H. J., and W. Helfrich. 1976. The curvature elasticity of fluid membranes. *J. Phys. France.* 37:1335–1345.

Deuticke, B. 1968. Transformation and restoration of biconcave shape of human erythrocytes induced by amphiphilic agents and changes of ion environment. *Biochim. Biophys. Acta.* 163:494–500.

Evans, E., and R. Skalak. 1980. Mechanics and Thermodynamics of Biomembranes. CRC Press, Boca Raton, FL. 1–254.

Fischer, T. M. 1992. Bending stiffness of lipid bilayers. III. Gaussian curvature. *J. Phys. II (France).* 2:337–343.

Fischer, T. M. 1993. Bending stiffness of lipid bilayers. V. Comparison of two formulations. *J. Phys. II (France).* 3:1795–1805.

Fournier, J. B. 1996. Nontopological saddle-splay and curvature instabilities from anisotropic membrane inclusions. *Phys. Rev. Lett.* 76: 4436–4439.

Fournier, J. B., and P. Galatola. 1997. Tubular vesicles and effective fourth-order membrane elastic theories. *Europhys. Lett.* 39:225–230.

Fujii, T., T. Sato, A. Tamura, M. Wakatsuki, and Y. Kanaho. 1979. Shape changes of human erythrocytes induced by various amphipathic drugs acting on the membrane of the intact cell. *Biochem. Pharmacol.* 28: 613–620.

Hägerstrand, H., and B. Isomaa. 1989. Vesiculation induced by amphiphiles in erythrocytes. *Biochim. Biophys. Acta.* 982:179–186.

Hägerstrand, H., and B. Isomaa. 1991. Amphiphile-induced antihaemolysis is not causally related to shape changes and vesiculation. *Chem. Biol. Interact.* 79:335–347.

Hägerstrand, H., and B. Isomaa. 1992. Morphological characterization of exovesicles and endovesicles released from human erythrocytes following treatment with amphiphiles. *Biochim. Biophys. Acta.* 1109:117–126.

Heerklotz, H., H. Binder, G. Lantzsch, G. Klose, and A. Blume. 1997. Lipid/detergent interaction thermodynamics as a function of molecular shape. *J. Phys. Chem. B.* 101:639–645.

Heerklotz, H., H. Binder, and H. Schmiedel. 1998. Excess enthalpies of mixing in phospholipid-additive membranes. *J. Phys. Chem. B.* 102: 5363–5368.

Iglič, A., and H. Hägerstrand. 1999. Amphiphile-induced spherical microexovesicles correspond to an extreme local area difference between two monolayers of the membrane bilayer. *Med. Biol. Eng. Comp.* 37: 125–129.

Iglič, A., V. Kralj-Iglič, P. Peterlin, and H. Hägerstrand. 1998. Cylindrical shapes of red blood cell microexovesicles. *Cell. Mol. Biol. Lett.* 3:443–448.

Isomaa, B., H. Hägerstrand, and G. Paatero. 1987. Shape transformations induced by amphiphiles in erythrocytes. *Biochim. Biophys. Acta.* 899: 93–103.

Israelachvili, J. N. 1985. Intermolecular and Surface Forces. Academic Press, London. 1–296.

Kralj-Iglič, V., V. Heinrich, S. Svetina, and B. Žekš. 1999. Free energy of closed membrane with anisotropic inclusions. *Eur. Phys. J. B.* 10:5–8.

Kralj-Iglič, V., S. Svetina, and B. Žekš. 1996. Shapes of bilayer vesicles with membrane embedded molecules. *Eur. Biophys. J.* 24:311–321.

Leibler, S. 1986. Curvature instability in membranes. *J. Phys. (Paris).* 45:507–516.

Lipowsky, R. 1991. The conformation of membranes. *Nature.* 349: 475–481.

Markin, V. S. 1981. Lateral organization of membranes and cell shapes. *Biophys. J.* 36:1–19.

Miao, L., U. Seifert, M. Wortis, and H. G. Döbereiner. 1994. Budding transitions of fluid-bilayer vesicles: the effect of area difference elasticity. *Phys. Rev. E.* 49:5389–5400.

Otten, D., L. Löbbecke, and K. Beyer. 1995. Stages of the bilayer-micelle transition in the system phosphatidylcholine-C12E8 as studied by deuterium and phosphorus NMR, light scattering, and calorimetry. *Biophys. J.* 68:584–597.

Safinya, C. R. 1997. Biomolecular materials: structure, interactions and higher order self-assembly. *Coll. Surf. A.* 128:183–195.

Seifert, U. 1993. Curvature-induced lateral phase segregation in two-component vesicles. *Phys. Rev. Lett.* 70:1335–1338.

Sheetz, M. P., and S. J. Singer. 1974. Biological membranes as bilayer couples. A molecular mechanism of drug-erythrocyte interactions. *Proc. Natl. Acad. Sci. USA.* 71:4457–4461.

Sheetz, M. P., and S. J. Singer. 1976. Equilibrium and kinetic effects of drugs on the shape of human erythrocytes. *J. Cell. Biol.* 70:247–251.

Svetina, S., A. Iglič, and B. Žekš. 1994. On the role of the elastic properties of closed lamellar membranes in membrane fusion. *Ann. N.Y. Acad. Sci.* 416:179–191.

Svetina, S., and B. Žekš. 1989. Membrane bending energy and shape determination of phospholipid vesicles and red blood cells. *Eur. Biophys. J.* 17:101–111.

Thurmond, R. L., D. Otten, M. F. Brown, and K. Beyer. 1994. Structure and packing of phosphatidylcholines in lamellar and hexagonal liquid-crystalline mixtures with a nonionic detergent: a wide-line deuterium and phosphorus-31 NMR study. *J. Phys. Chem.* 98:972–983.

Waugh, R. E. 1996. Elastic energy of curvature-driven bump formation on red blood cell membrane. *Biophys. J.* 70:1027–1035.

Wenk, M. R., T. Alt, A. Seeling, and J. Seelig. 1997. Octyl-β-D-glucopyranoside partitioning into lipid bilayers: thermodynamics of binding and structural changes of the bilayer. *Biophys. J.* 72:1719–1731.